Carrier dynamics in InGaAs with embedded ErAs nanoislands

Abul K. Azad,[1,a)] Rohit P. Prasankumar,[1] Diyar Talbayev,[1] Antoinette J. Taylor,[1] Richard D. Averitt,[2] Joshua M. O. Zide,[3] Hong Lu,[4] Arthur C. Gossard,[4] and John F. O'Hara[1]

[1]*MPA-CINT, Los Alamos National Laboratory, Los Alamos, New Mexico 87545, USA*
[2]*Department of Physics, Boston University, 590 Commonwealth Avenue, Boston, Massachusetts 02215, USA*
[3]*Electrical and Computer Engineering, University of Delaware, Delaware 19716, USA*
[4]*Materials Department, University of California, Santa Barbara, California 93106, USA*

(Received 21 July 2008; accepted 5 September 2008; published online 24 September 2008)

Using time-resolved optical-pump terahertz-probe spectroscopy, we study the ultrafast carrier dynamics in $In_{0.53}Ga_{0.47}As$:ErAs, a potential candidate for 1550 nm based terahertz photoconductive detectors. Material growth is performed by codepositing ErAs nanoislands with Be-compensated InGaAs on an InP:Fe substrate using molecular beam epitaxy. The material shows a rapid photoconductivity response following optical excitation. Photoexcitation with $\sim 0.5\ \mu J/cm^2$ 800 nm femtosecond laser pulses yields a 3.2 ps carrier lifetime in optical-pump terahertz-probe experiments. We also measure the carrier lifetime using a 1550 nm femtosecond optical pump-probe system, and it is found to agree well with the terahertz measurements. These short lifetimes demonstrate significant potential for implementing terahertz systems using telecommunication based technologies. © *2008 American Institute of Physics*. [DOI: 10.1063/1.2989127]

Despite a growing demand for terahertz applications, such as imaging, interchip communication, short range wireless, and nondestructive spectroscopy,[1–3] terahertz technology still suffers from a serious lack of functional devices, in particular compact and efficient generators and detectors. Photoconductive antennas are prevalent as high-performance terahertz devices that utilize the optoelectronic response of semiconductors to make terahertz generation and detection possible with commercially available 800 nm femtosecond lasers. However, the major factor that severely limits their wide applicability is the scarcity of suitable semiconductors having an ultrafast carrier lifetime ($\sim$1 ps), low dark current, and simultaneous compatibility with compact powerful ultrafast laser sources. Traditionally, radiation damaged silicon-on-sapphire (RD-SOS) or low temperature grown GaAs (LT-GaAs) is used for photoconductive antennas compatible with 800 nm femtosecond lasers. However, tuning the carrier lifetimes of RD-SOS and LT-GaAs is not exact because of the limitations in fabrication,[4–6] and this can result in a degradation of device performance through other parameters (dark current, mobility, etc.). Furthermore, neither semiconductor is amenable to operation with 1550 nm (telecom) lasers, though such lasers offer the advantages of low cost and maintenance, small footprints, excellent noise performance, and naturally low-dispersion pulse delivery via optical fibers. Such lasers are typically frequency doubled to operate terahertz systems, but this severely reduces the available optical power at the terahertz devices. In addition, since doubling occurs at the laser, this approach does not take advantage of low-dispersion fiber delivery. To benefit from 1550 nm technology, it is essential to explore alternative semiconductors for terahertz detection. Some progress has already been made with 1550-nm-based photoconductive switches fabricated on various InGaAs substrates.[7–9] In this letter, we use optical-pump terahertz-probe (OPTP) spectroscopy and 1550 nm optical pump-probe measurements to study the carrier dynamics of a promising alternative: bulk InGaAs:ErAs formed by codepositing embedded ErAs nanoislands into an InGaAs matrix. We measured carrier relaxation times as short as 2.6 ps, suggesting that this material may be suitable for terahertz detection antennas that are gated by ultrashort 1550 nm pulses.

The properties of self-assembled ErAs nanoislands embedded in GaAs and InGaAs have been investigated with great interest for ultrafast applications.[10–12] GaAs:ErAs superlattices have high mobility (μ=4324 $cm^2\ V^{-1}\ S^{-1}$) and short ($\sim$800 fs) carrier lifetimes[11] and have been shown to produce excellent 800 nm terahertz detectors.[13] Due to its smaller bandgap, InGaAs:ErAs is suitable for telecom wavelength applications. InGaAs:ErAs superlattices have room temperature mobility varying from 200 to 1800 $cm^2\ V^{-1}\ S^{-1}$, and they can have carrier lifetimes as short as 0.3 ps (Ref. 12) for optimum superlattice period and doping.

The $In_{0.53}Ga_{0.47}As$:ErAs sample used in this work was grown by molecular beam epitaxy on a $\langle 100 \rangle$ semi-insulating InP:Fe substrate with a 100 nm InAlAs buffer layer at a temperature of 450 °C. The InGaAs and ErAs were deposited simultaneously with a growth rate of about 2 μm/h to form the 2-μm-thick bulk layer of InGaA:ErAs. During growth, the ErAs forms into nanoparticles (traps) in the InGaAs matrix with an average size of $\sim$2 nm. The estimated trap density is about $1 \times 10^{18}\ cm^{-3}$. Beryllium compensation is also used to minimize the dark current and results in a *n*-type free carrier concentration of about $1.3 \times 10^{15}\ cm^{-3}$. Figure 1 (inset) shows a schematic cross section of the sample used for the measurements.

This codeposited growth offers several potential advantages over the superlattice growth used in previous GaAs:ErAs studies.[11,13] First, superlattice growth requires numerous interruptions,[10] while codeposited growth does not. Since small layer spacings are desirable for short lifetimes,[10] these interruptions ($\sim$30 s/period) can increase deposition times substantially. The other significant advantage of codeposited materials is the decreased average spac-

a)Electronic mail: aazad@lanl.gov.

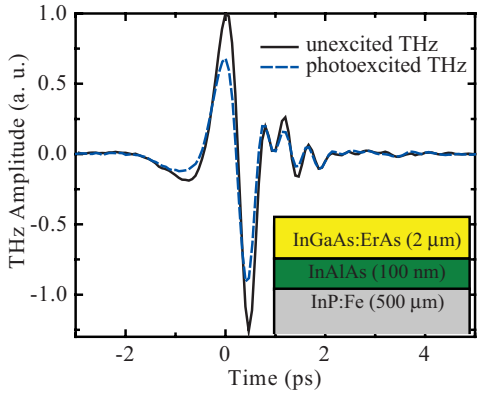

FIG. 1. (Color online) Time-dependent terahertz pulses transmitted through InGaAs:ErAs samples. The black and the blue curves represent the transmitted terahertz pulses before and after optical excitation (~5 $\mu J/cm^2$), respectively. Amplitudes are normalized to the unexcited pulse amplitude maximum. The inset shows a cross-sectional view of the sample.

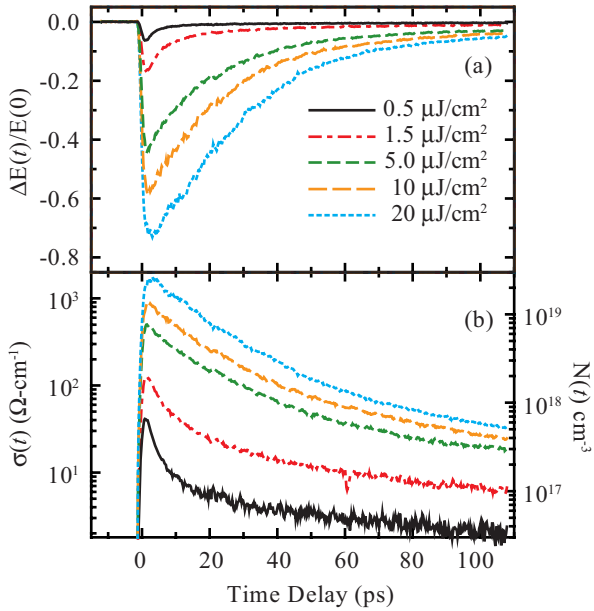

FIG. 2. (Color online) OPTP measurements at various pump fluences with 800 nm pump. (a) Pump-induced transmission change normalized to the unexcited terahertz amplitude maximum $\Delta E(t)/E(0)$ as a function of pump delay. (b) Photoinduced conductivity $\sigma(t)$ (left y-axis) and carrier density $N(t)$ (right y-axis) vs time delay.

ing between particles, again desirable for short lifetimes. In a superlattice, the average distance to a particle is $L/2$ (where L is the layer spacing, typically ~20–50 nm), while the spacing in the codeposited material scales as $N^{-1/3}$, where N is the ErAs trap density. Our codeposited sample has an average spacing of ~10 nm.

The OPTP experiment utilizes a 1 kHz regeneratively amplified Ti:Sapphire laser capable of generating 3.2 mJ, 50 fs pulses at 800 nm. Part of the output laser power is used for terahertz generation and detection using ZnTe crystals via the electro-optic effect.[14] The system generates a ~2.5 THz bandwidth beam that propagates normally through the sample and has a frequency-independent diameter of 4 mm at the focus.[11] The remainder of the optical power passes through a variable attenuator to form a ~10 mm diameter illumination spot at the sample. Measurements were performed at room temperature and in a dry air environment. Optical pump fluences of 0.5, 1.5, 5.0, 10, and 20 $\mu J/cm^2$ were used to excite the sample. The penetration depth of 800 nm light into InGaAs is ~200 nm, so the 2 μm thickness is sufficient to absorb the entire incident pump light.

Figure 1 shows typical time-domain terahertz pulses following passage through the InGaAs:ErAs sample before (solid) and after (dashed) optical excitation. Here, the photoexcited terahertz pulse is recorded 5 ps after pump pulse arrival. Upon optical excitation free carriers generated within the InGaAs attenuate the transmitted terahertz pulses. Figure 2(a) shows the normalized change in the terahertz peak electric field $\Delta E(t)/E_0$ as a function of delay between optical pump and terahertz probe pulses. Here, $\Delta E(t)$ is the time-dependent differential change in the terahertz peak amplitude and E_0 is the peak amplitude of terahertz pulses without optical excitation. Clearly, the terahertz transmission decreases as the increasing pump fluence creates more photocarriers. The peak transmission decreased to about 75% of its maximum value when the sample was illuminated with a fluence of 20 $\mu J/cm^2$. The evolution of $\Delta E(t)/E_0$ following photoexcitation shows a characteristic recovery time that also depends on the pump fluence. $\Delta E(t)/E_0$ approaches zero as the time delay between optical and terahertz pulse increases, indicating that photocarriers are being trapped by the available ErAs inclusions.

Because of the small penetration depth at 800 nm, we consider the photoexcited layer of InGaAs:ErAs as a highly conductive film on a semi-infinite insulating substrate. Following photoexcitation, the conductivity of such a film has a time dependence, which can be expressed as[11,15]

$$\sigma(t) = \frac{1+n}{Z_0 d}\left[\frac{1}{1+\Delta E(t)/E_0} - 1\right], \tag{1}$$

where $Z_0 = 377\ \Omega$ is the impedance of free space, $n = 3.5$ is the measured refractive index of InGaAs:ErAs at terahertz frequencies, and d is the optical penetration depth of the pump beam inside the film. The time-dependent photoinduced conductivity is shown in Fig. 2(b). This conductivity is about 3.5 times larger than that of the GaAs:ErAs superlattices,[11] due in part to the shorter penetration depth of 800 nm light in InGaAs and the associated higher carrier density. The photoinduced carrier density $N(t)$ is directly related to the conductivity via $\sigma(t) = N(t)\mu e$, where μ is the mobility and e is the fundamental electronic charge. Within the limit of the optical fluence used in this work, it is justifiable to consider the mobility as constant and equal to the measured value of 384 $cm^2/V\,s$ by Hall effect measurements. Figure 2(b) shows the extracted photocarrier density (right scale) from the measured data. Our maximum photocarrier density for 20 $\mu J/cm^2$ is 2×10^{19} cm^{-3}, which is consistent with the number of available photons being completely absorbed in ~200 nm. The photocarrier density shows an exponential decay with time due to carrier trapping in the ErAs nanoislands.

Equation (1) suggests that the transient terahertz transmission change $\Delta E(t)$ is proportional to the number of free photocarriers. Figure 3(a) shows the normalized $|\Delta E(t)|$ as a function of pump delay for all fluences. The transient terahertz change $\Delta E(t)$ can be fit (smooth gray lines) by the convolution of a 1.3-ps Gaussian experimental response (the terahertz pulse duration) and a biexponential decay function.[16] The biexponential represents two characteristic decay times involved in the relaxation process. The fast de-

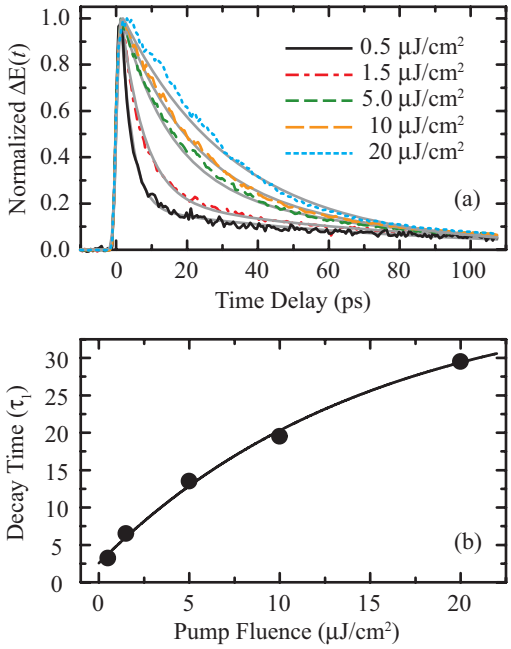

FIG. 3. (Color online) (a) Transmission change $|\Delta E(t)|$ normalized to unity at different fluences. Smooth gray curves show the biexponential fit. (b) Fluence dependent carrier lifetimes: black dots are the measured values and the solid line is the exponential growth fitting.

cay component τ_1 near $t=0$ varies with the pump fluence and represents rapid photocarrier capture by the ErAs traps. Figure 3(b) shows the corresponding fitting values of the fast decay time τ_1 as a function of the pump fluence (black dots). The shortest $\tau_1=3.2$ ps was obtained when the optical fluence was 0.5 $\mu J/cm^2$. However, τ_1 increases with pump fluence. This is caused by trap saturation occurring when the density of photocarriers exceeds the density of available traps ($\sim 1\times 10^{18}$ cm^{-3}). The solid curve shows that a simple exponential $\tau_1=-36.45e^{-P/15}+39.05$ (where P is the fluence) captures the behavioral trend of carrier lifetime versus fluence. The longer decay component $\tau_2 \sim 75$ ps and is independent of the pump fluence. Though the longer decay is still under investigation, it may be due to trapping at growth defects, shallow defect states near the ErAs particles, or Be-based complexes.

Since InGaAs:ErAs is an appropriate material for ultrafast switches at telecom wavelengths, we also measured the photocarrier lifetime using 1550 nm optical pump-probe reflection measurements. We used an IMRA brand femtosecond fiber laser system (BX-60) that generates ~60 fs pulses with an average output power of 80 mW. Most of the power is used to pump the sample and the remainder is used to probe the reflection change (ΔR), which is proportional to the generated photocarrier density.[16] We performed the measurements for two different optical fluences, 20 nJ/cm^2 (blue curve) and 5 nJ/cm^2 (red curve), as shown in Fig. 4. The normalized change in reflectivity ($\Delta R/R$) is approximately 10^{-5}, which translates into an estimated photocarrier density of $\sim 10^{14}$ cm^{-3}, much lower than the available trap density. We note that the penetration depth of 1550 nm light is ~2 μm in InGaAs:ErAs. These data can be modeled using a 100 fs Gaussian response function together with a single exponential having a characteristic decay time of 2.6 ps. There is no apparent difference in decay times for the 20

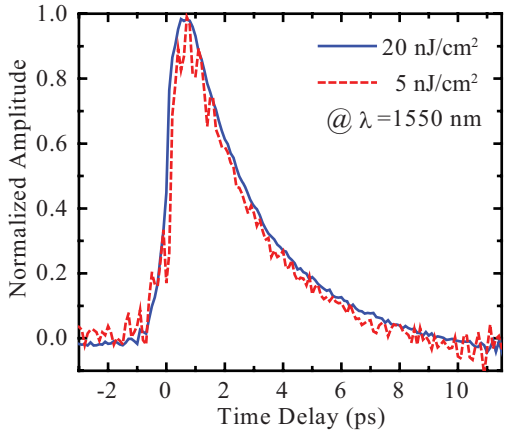

FIG. 4. (Color online) Transient reflectivity changes ($|\Delta R|$) measured in 1550 nm optical pump-probe experiments as a function of pump delay. For comparison $|\Delta R|$ is normalized to unity.

and 5 nJ/cm^2 excitations. We can also estimate the carrier lifetime from the exponential fitting [solid curve in Fig. 3(b)] of τ_1 versus fluence, obtained by OPTP. This is ~2.6 ps, which agrees very well with our optical-pump optical-probe measurements. Again, this indicates that the photocarrier relaxation process is dominated by the ErAs trapping time under low fluence excitation (<0.5 $\mu J/cm^2$). Though this InGaAs:ErAs sample has a longer carrier lifetime than previous GaAs:ErAs superlattice samples,[11] there is still some degree of lifetime reduction available by increasing the density of ErAs traps.

In conclusion, we have measured the carrier relaxation dynamics of codeposited InGaAs:ErAs. Our 800 nm OPTP measurements show carrier lifetimes of ~3 ps when excited with low fluence. This is confirmed by optical pump-probe measurements using a 1550 nm pulsed fiber laser. This material has a high potential for use in photoconductive terahertz detectors compatible with compact telecommunication-wavelength lasers. Our measurements also provide an estimate of optical fluence limitations and their relation to maximizing terahertz bandwidth.

This work was performed in part at the Center for Integrated Nanotechnologies, Los Alamos National Laboratory.

[1] *Sensing with Terahertz Radiation*, edited by D. M. Mittleman (Springer, Berlin, 2003).
[2] J. F. O'Hara and D. Grischkowsky, Opt. Lett. **27**, 1070 (2002).
[3] A. K. Azad, J. Han, and W. Zhang, Appl. Phys. Lett. **88**, 021103 (2006).
[4] S. Gupta and J. F. Whitaker, IEEE J. Quantum Electron. **28**, 2464 (1992).
[5] F. E. Doany, D. Grischkowsky, and C.-C. Chi, Appl. Phys. Lett. **50**, 460 (1987).
[6] D. C. Look, J. Appl. Phys. **70**, 3148 (1991).
[7] A. Takazato, M. Kamakura, T. Matsui, J. Kitagawa, and Y. Kadoya, Appl. Phys. Lett. **90**, 101119 (2007).
[8] M. Suzuki and M. Tonouchi, Appl. Phys. Lett. **86**, 051104 (2005).
[9] L. Meignien, J. Mangeney, P. Crozat, L. Duvillaret, and M. Hanna, Appl. Phys. Lett. **92**, 131103 (2008).
[10] C. Kadow, S. B. Fleischer, J. P. Ibbetson, J. E. Bowers, A. C. Gossard, J. W. Dong, and C. J. Palmstrom, Appl. Phys. Lett. **75**, 3548 (1999).
[11] R. P. Prasankumar, A. Scopatz, D. J. Hilton, A. J. Taylor, and R. D. Averitt, Appl. Phys. Lett. **86**, 201107 (2005).
[12] D. C. Driscoll, M. P. Hanson, A. C. Gossard, and E. R. Brown, Appl. Phys. Lett. **86**, 051908 (2005).
[13] J. F. O'Hara, J. M. O. Zide, A. C. Gossard, A. J. Taylor, and R. D. Averitt, Appl. Phys. Lett. **88**, 251119 (2006).
[14] Q. Wu, M. Litz, and X.-C. Zhang, Appl. Phys. Lett. **68**, 2924 (1996).
[15] K. P. H. Lui and F. A. Hegmann, Appl. Phys. Lett. **78**, 3478 (2001).
[16] F. E. Doany and D. Grischkowsky, Appl. Phys. Lett. **52**, 36 (1988).